Switching Fuzzy Energy Method Optimized by Genetic Algorithm for Controlling Underactuated Manipulators

Kiyotaka Izumi, Keisuke Ichida, and Keigo Watanabe
Department of Advanced Systems Control Engineering,
Graduate School of Science and Engineering,
Saga University, 1-Honjomachi, Saga 840-8502, Japan
E-mail: {izumi, watanabe}@me.saga-u.ac.jp

***Abstract*—Underactuated manipulators can move smoothly and quickly by their dynamical characteristics, because they have some passive joints. One of control methods for such underactuated manipulators is known as a switching control which selects a partially-stable controller using a switching rule. In this paper, we propose a switching rule method based on fuzzy energy regions for the switching control. Furthermore, parameters related on fuzzy energy regions are designed by a genetic algorithm (GA). The effectiveness of the switching fuzzy energy method is demonstrated with some simulations.**

I. Introduction

Underactuated manipulators have to be controlled by following a restricted way that the number of actuators is less than the number of generalized coordinates, because they have some passive joints [1], [2], [3]. Underactuated manipulators can perform more smooth and quick motion than standard manipulators which consist of whole active joints.

As a control method for underactuated systems, authors have already proposed a switching control, in which some partly stable controllers were designed by computed torque method and the switching low was obtained as the index of controller directly by fuzzy reasoning [4]. A logic based switching method using energy regions [5] is also proposed for a nonholonomic system without drift term [6].

In this paper, we propose a logic based switching mechanism using fuzzy energy region. Boundary curves to separate a energy region into some energy subregions are constructed by fuzzy reasoning. Therfore, fuzzy related parameters are optimized by genetic algorithm (GA). The present method is applied to an underactuated system with drift term such as an 2-DOF planar manipulator which has only one active joint. The effectiveness of the present method is illustrated with some simulations.

II. Underactuated Manipulator

Figure 1 shows a two-link underactuated manipulator, in which the second joint is constructed of a passive joint. Here, τ_1 denotes the applying torque of 1st joint, θ_i denotes the angle of ith link, m_i denotes the mass of ith link, l_{gi} denotes the distance from the joint to the center of mass of ith link, I_i denotes the moment of inertia of ith link, and μ_i denotes the coefficient of viscous friction. The dynamical model of an underactuated manipulator is given as follows:

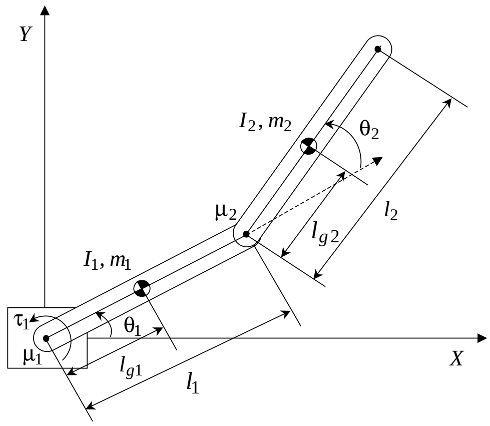

Fig. 1. Model of 2-link underactuated manipulator

$$M(\boldsymbol{\theta})\ddot{\boldsymbol{\theta}} + \boldsymbol{h}\left(\boldsymbol{\theta},\, \dot{\boldsymbol{\theta}}\right) = \boldsymbol{\tau} \tag{1}$$

where

$$\begin{aligned}
\boldsymbol{\theta} &= [\theta_1 \;\; \theta_2]^T \\
\boldsymbol{\tau} &= [\tau_1 \;\; 0]^T \\
M(\boldsymbol{\theta}) &= \begin{bmatrix} M_{11}(\boldsymbol{\theta}) & M_{12}(\boldsymbol{\theta}) \\ M_{12}(\boldsymbol{\theta}) & M_{22}(\boldsymbol{\theta}) \end{bmatrix} \\
M_{11}(\boldsymbol{\theta}) &= (m_1 l_{g2}^2 + m_2 l_1^2 + I_1) + (m_2 l_{g2}^2 + I_2) \\
&\quad + 2 m_2 l_1 l_{g2} \cos\theta_2 \\
M_{12}(\boldsymbol{\theta}) &= (m_2 l_{g2}^2 + I_2) + m_2 l_1 l_{g2} \cos\theta_2 \\
M_{22}(\boldsymbol{\theta}) &= m_2 l_{g2}^2 + I_2 \\
\boldsymbol{h}\left(\boldsymbol{\theta},\, \dot{\boldsymbol{\theta}}\right) &= \left[h_1\left(\boldsymbol{\theta},\, \dot{\boldsymbol{\theta}}\right) \; h_2\left(\boldsymbol{\theta},\, \dot{\boldsymbol{\theta}}\right)\right]^T \\
h_1\left(\boldsymbol{\theta},\, \dot{\boldsymbol{\theta}}\right) &= -(m_2 l_1 l_{g2})(2\dot{\theta}_1\dot{\theta}_2 + \dot{\theta}_2^2)\sin\theta_2 + \mu_1\dot{\theta}_1 \\
h_2\left(\boldsymbol{\theta},\, \dot{\boldsymbol{\theta}}\right) &= m_2 l_1 l_{g2} \dot{\theta}_1^2 \sin\theta_2 + \mu_2\dot{\theta}_2
\end{aligned}$$

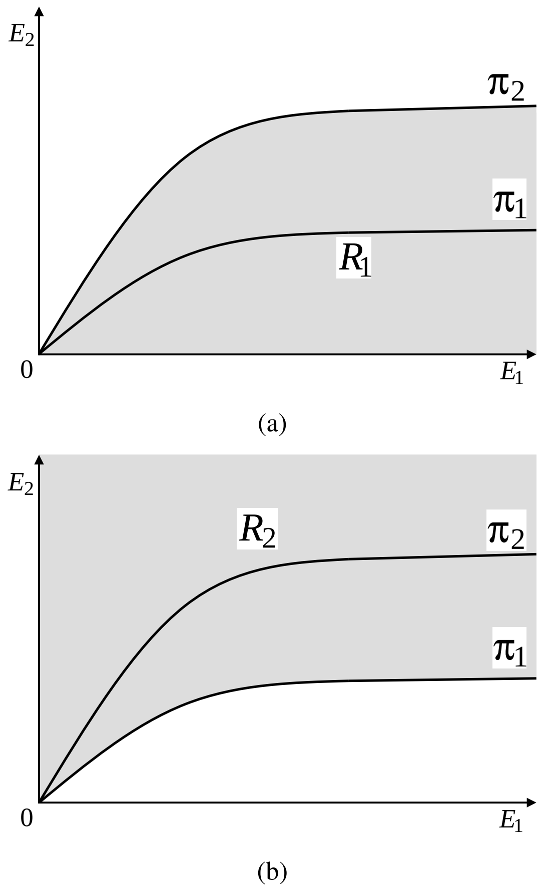

Fig. 2. Subregions of energy

III. Fuzzy Region Based Switching Control

A. Partly stable controller

Equation (1) can be described by

$$
\begin{aligned}
\ddot{\theta}_1 &= -\frac{M_{22}(\boldsymbol{\theta})}{D} h_1\left(\boldsymbol{\theta},\, \dot{\boldsymbol{\theta}}\right) + \frac{M_{12}(\boldsymbol{\theta})}{D} h_2\left(\boldsymbol{\theta},\, \dot{\boldsymbol{\theta}}\right) \\
&\quad + \frac{M_{22}(\boldsymbol{\theta})}{D}\tau_1 \qquad (2) \\
\ddot{\theta}_2 &= \frac{M_{12}(\boldsymbol{\theta})}{D} h_1\left(\boldsymbol{\theta},\, \dot{\boldsymbol{\theta}}\right) - \frac{M_{11}(\boldsymbol{\theta})}{D} h_2\left(\boldsymbol{\theta},\, \dot{\boldsymbol{\theta}}\right) \\
&\quad - \frac{M_{12}(\boldsymbol{\theta})}{D}\tau_1 \qquad (3)
\end{aligned}
$$

where

$$D = M_{11}(\boldsymbol{\theta})\, M_{22}(\boldsymbol{\theta}) - M_{12}^2(\boldsymbol{\theta})$$

Here, it is found that we can design partly stable controllers for link 1 and link 2 using the computed torque method. The controller 1 to stabilize the link 1 is given by

$$
\begin{aligned}
\tau_1 &= \frac{D}{M_{22}(\boldsymbol{\theta})}\left(\ddot{\theta}_1^* + \frac{M_{22}(\boldsymbol{\theta})}{D} h_1\left(\boldsymbol{\theta},\, \dot{\boldsymbol{\theta}}\right)\right. \\
&\quad \left. - \frac{M_{12}(\boldsymbol{\theta})}{D} h_2\left(\boldsymbol{\theta},\, \dot{\boldsymbol{\theta}}\right)\right) \qquad (4) \\
\ddot{\theta}_1^* &= \ddot{\theta}_{d1} + K_{v1}\left(\dot{\theta}_{d1} - \dot{\theta}_1\right) + K_{p1}\left(\theta_{d1} - \theta_1\right)
\end{aligned}
$$

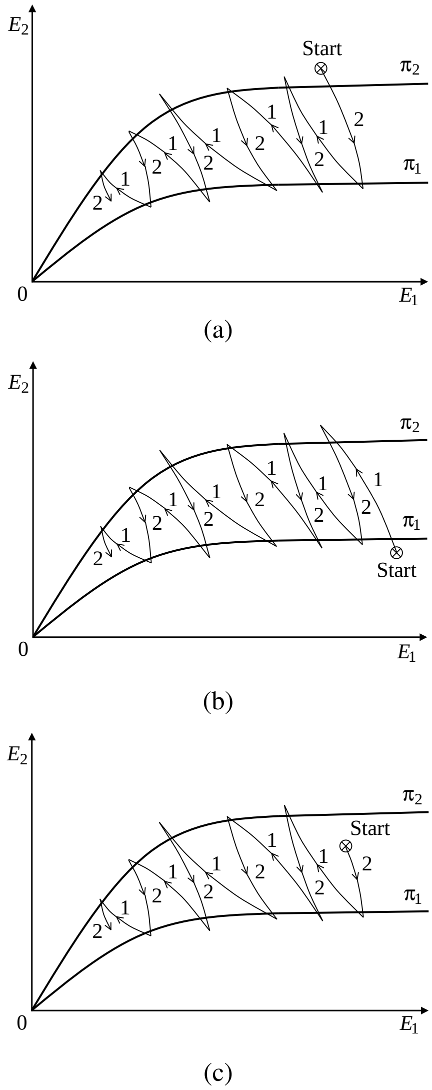

Fig. 3. Ideal convergence situations of switching method with two controllers

and the controller 2 to stabilize the link 2 is given by

$$
\begin{aligned}
\tau_1 &= -\frac{D}{M_{12}(\boldsymbol{\theta})}\left(\ddot{\theta}_2^* - \frac{M_{12}(\boldsymbol{\theta})}{D} h_1\left(\boldsymbol{\theta},\, \dot{\boldsymbol{\theta}}\right)\right. \\
&\quad \left. + \frac{M_{11}(\boldsymbol{\theta})}{D} h_2\left(\boldsymbol{\theta},\, \dot{\boldsymbol{\theta}}\right)\right) \qquad (5) \\
\ddot{\theta}_2^* &= \ddot{\theta}_{d2} + K_{v2}\left(\dot{\theta}_{d2} - \dot{\theta}_2\right) + K_{p2}\left(\theta_{d2} - \theta_2\right)
\end{aligned}
$$

where the desired vector of $\boldsymbol{\theta}$ is defined as $\boldsymbol{\theta}_d = [\theta_{d1} \;\; \theta_{d2}]^T$, in which the proportional gain of the controller i is K_{pi} and the derivative gain of the controller i is K_{vi}.

B. Logic based switching method

Energy of each link is defined by

$$E_i \triangleq e_i^2 + \dot{e}_i^2, \quad i = 1,\ 2 \qquad (6)$$

with

$$
\begin{aligned}
e_i &= \theta_{di} - \theta_i \\
\dot{e}_i &= \dot{\theta}_{di} - \dot{\theta}_i
\end{aligned}
$$

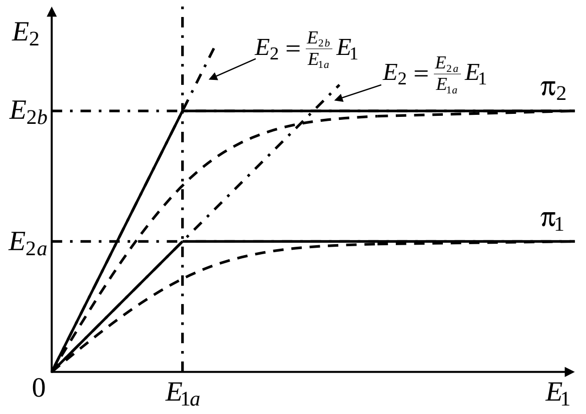

Fig. 4. Approximation of regions for a logical switching

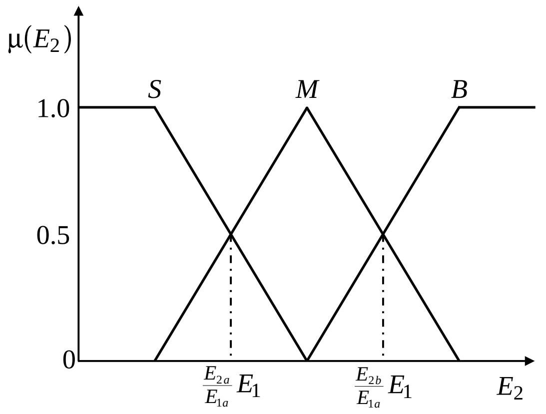

Fig. 5. Membership functions for $E_1 \leq E_{1a}$

Energy plane is composed of E_i as shown in Fig. 2. In Fig. 2, π_i is a boundary curve which determines the subregion of energy to use a partly stable controller, and is plotted by an exponential curve. The region R_i with gray shadow is the subregion to which the controller i is applied. Ideal responses of energy are illustrated with Fig. 3, when assuming that E_i is decreased monotonously while the controller i is selected. In Fig. 3(a), the initial controller is the controller 2, because the initial point of energy locates at the subregion R_2. Even though E_2 is decreased, E_1 is increased until the controller 1 will be selected, depending on the location of current energy. When the controller 1 is selected, energy responses become the opposite situation. Consequently, each energy converges to zero with switching partly stable controllers. Fig. 3(b) is illustrated with the case that the initial point of energy locates at the subregion R_1. Fig. 3(c) is illustrated with the case that the initial point of energy locates at the overlapped region between R_1 and R_2. It is assumed that the controller having the biggest index number has to be selected in the overlapped case. In this example, the controller 2 is selected.

C. Fuzzy energy region method

If a boundary curve comprises an exponential function, we can suitably design it with the amplitude and the time constant of a step-response. It is difficult to design such parameters of the function in advance, because we can't theoretically analyze them depending on the switching control. Therefore, we propose a fuzzy energy region based switching control method. At first, boundary curves are approximated by several straight-lines as shown in Fig. 4. After these approximations, fuzzy sets for E_2 can be defined for $E_1 \leq E_{1a}$ and $E_1 > E_{1a}$ cases as shown in Fig. 5 and Fig. 6. E_{1a}, E_{2a} and E_{2b} are design parameters of fuzzy sets. In order to realize ideal energy responses as shown in Fig. 3, fuzzy rules are given as follows:

Rule 1	:	If $E_2 = S$	then $s_1 = 1$		
Rule 2	:	If $E_2 = M$	and $\phi_{t-1} = 1$	then $s_2 = 1$
Rule 3	:	If $E_2 = M$	and $\phi_{t-1} = 2$	then $s_3 = 2$
Rule 4	:	If $E_2 = B$	then $s_4 = 2$		

Note that, a parameter ϕ_{t-1} which means the index of controller for one-step delay, is introduced, because one-step delayed controller must be retained in the overlapped energy region according to ideal energy response as shown in Fig. 3. s_i is the index of controller that must be used in the fuzzy rule i.

The advantage of the present method is to set design parameters roughly, comparing to the logic based switching method, because the boundary curves have fuzziness to use the present fuzzy reasoning.

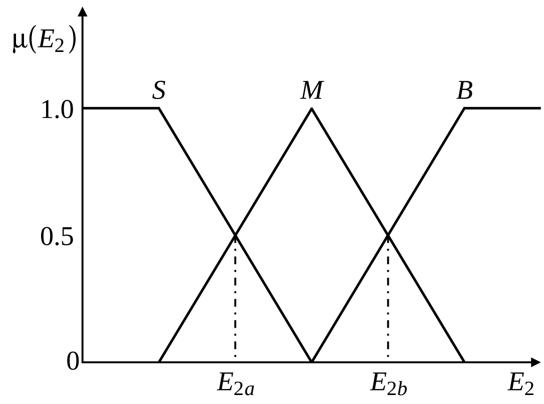

Fig. 6. Membership functions for $E_1 > E_{1a}$

TABLE I
GA OPERATIONS AND METHODS

GA operations	Method
Selection for crossover	Tournament strategy with 3 individuals
Crossover	Uniform crossover with probability 0.6
Probability of mutation	1/96
Alternation	Elite strategy with 10 individuals

IV. Optimization of Design Parameters by GA

The present method has the same difficulty to design parameters in advance as the logic based switching method. Here, we discuss about the design parameters of fuzzy rules using GA. These parameters are E_{1a}, E_{2a} and E_{2b}. Each parameter is encoded by 32 [bit], then the size of an individual is 96 [bit]. The searching domain of each parameter is set from 0.1 to 15.0.

TABLE II
SETTING PARAMETERS OF SIMULATIONS

Conditions	Setting value
Simulation time	30 [s]
Sampling interval	0.01 [s]
Mass of each link	$m_1 = 0.582$ [kg], $m_2 = 0.079$ [kg]
Length of each link	$l_1 = 0.4$ [m], $l_2 = 0.22$ [m]
Distance between center of gravity and each joint	$l_{g1} = 0.2$ [m] $l_{g2} = 0.11$ [m]
Coefficient of viscous friction of each joint	$\mu_1 = 0$ [Ns/m^2] $\mu_2 = 0.02$ [Ns/m^2]
Gains of controller 1	$K_{p1} = 1, K_{v1} = 1$
Gains of controller 2	$K_{p2} = 1, K_{v2} = 12$
Desired state vector	$[0\ 0\ 0\ 0]^T$
1st initial state vector	$[0\ \pi/4\ 0\ 0]^T$
2nd initial state vector	$[\pi\ \pi/6\ 0\ 0]^T$

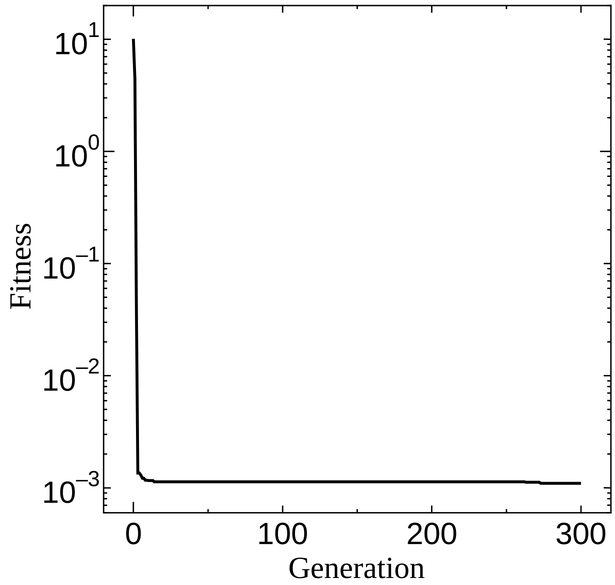

Fig. 7. Generation history of GA

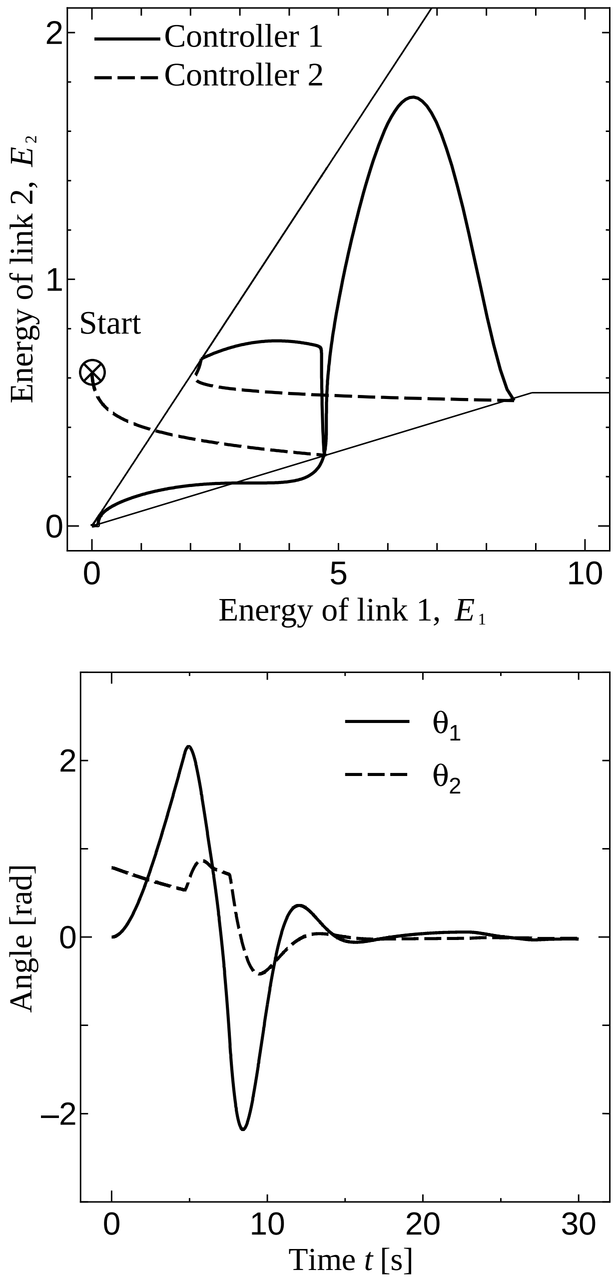

Fig. 8. Simulation results with training conditions using 1st initial state vector $[0\ \pi/4\ 0\ 0]$

Each parameter is decoded using gray code. The size of a population is 100. The maximum number of generations is 1000. GA operations used here are shown in Table I.

A fitness function is given by

$$f_c = \sum_{i=1}^{2} \sum_{j=2001}^{3000} \sum_{k=1}^{2} E_k(j) \tag{7}$$

where i is the index of simulation trials, j is the index of discrete times and k is the index of energy of each link. Simulation conditions to train fuzzy parameters are shown in Table II. Note that, the fitness function is not evaluated during a transition segment due to the dynamic characteristics of an underactuated system.

A training history in fitness function is shown in Fig. 7. The plotted maximum generation is 300 in Fig. 7, because the value of the fitness function remained the same value during from 276 to 1000 generations. Obtained parameters are $E_{1a} = 8.840$, $E_{2a} = 0.5406$ and $E_{2b} = 2.6942$. Figure 8 illustrates the energy response and the angler response of each link with the first initial state vector $[\pi\ \pi/4\ 0\ 0]$. The controller 2 was selected as the 1st controller, according to the initial state vector. Each energy converged to zero after some switchings. It was found from Fig. 8 that each angle converged to zero with a little oscillations. Simulation results using the 2nd initial state vector $[\pi\ \pi/6\ 0\ 0]$ are illustrated with Fig. 9. From this figure, we could verify the similar performance to Fig. 8. In this simulation, the controller 1 was selected for all the control durations without any switching of controllers. It was found from Fig. 8 and Fig. 9 that a kind of optimal subregion was obtained by

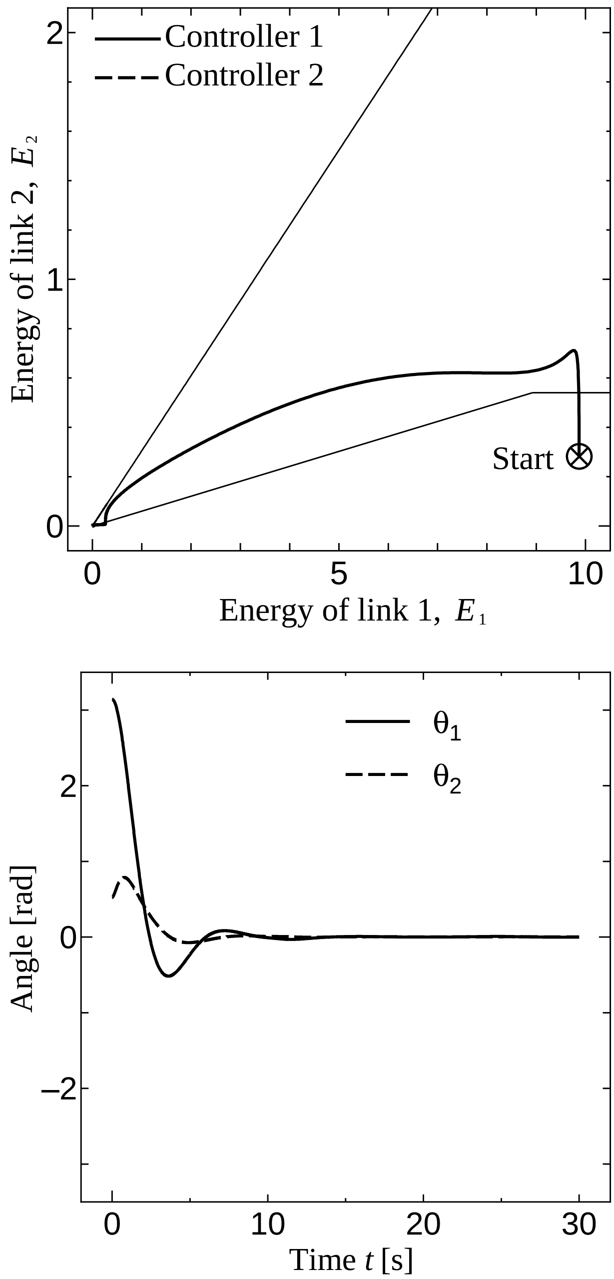

Fig. 9. Simulation results with training conditions using 2nd initial state vector $[\pi\ \pi/6\ 0\ 0]$

GA.

V. Simulations with Untrained Initial Sate Vectors

The obtained parameters are applied to the cases of untrained initial state vectors such as

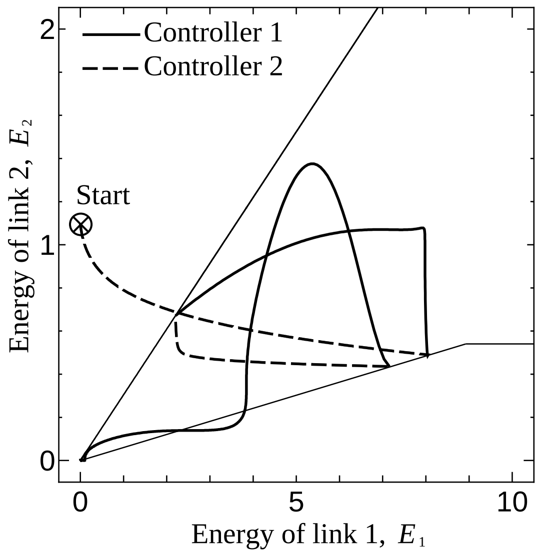

Fig. 10. Test simulation result with Case 1

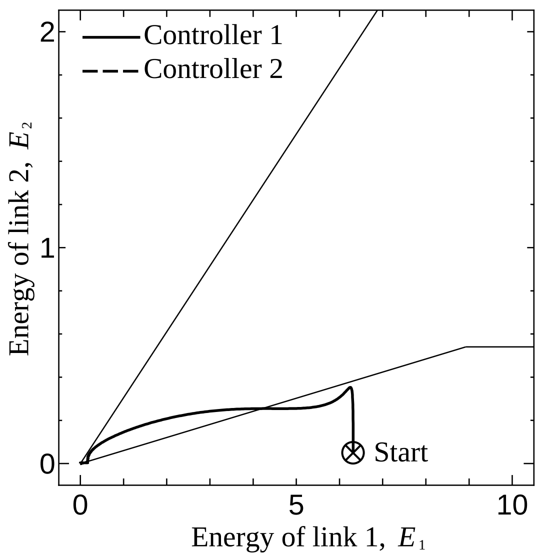

Fig. 11. Test simulation result with Case 2

$$
\begin{array}{lll}
\text{Case 1:} & \theta_1(0) = 0, & \theta_2(0) = \pi/3, \\
 & \dot{\theta}_1(0) = 0, & \dot{\theta}_2(0) = 0 \\
\text{Case 2:} & \theta_1(0) = 4\pi/5, & \theta_2(0) = \pi/14, \\
 & \dot{\theta}_1(0) = 0, & \dot{\theta}_2(0) = 0 \\
\text{Case 3:} & \theta_1(0) = \pi/2, & \theta_2(0) = -\pi/4, \\
 & \dot{\theta}_1(0) = 0, & \dot{\theta}_2(0) = 0 \\
\text{Case 4:} & \theta_1(0) = 5\pi/6, & \theta_2(0) = \pi/4, \\
 & \dot{\theta}_1(0) = 0, & \dot{\theta}_2(0) = 0
\end{array}
$$

Simulation results of energy trajectories are shown in Fig. 10 $\sim$ Fig. 13. Each energy converges to zero for all results, whose initial conditions are perturbed from the trained ones.

VI. Conclusions

We have proposed a logic based switching method using fuzzy energy region, in which fuzzy design parameters were

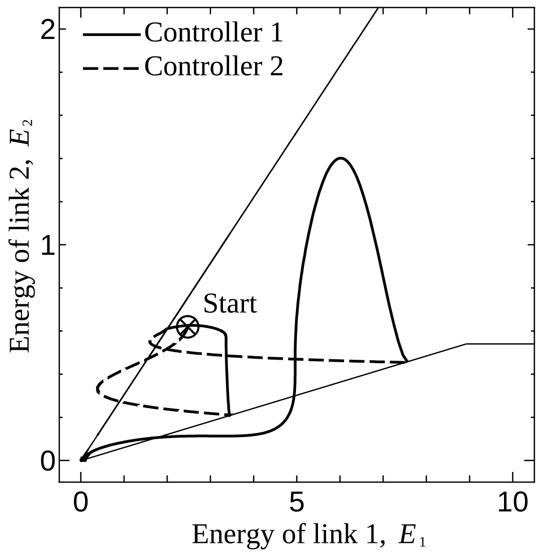

Fig. 12. Test simulation result with Case 3

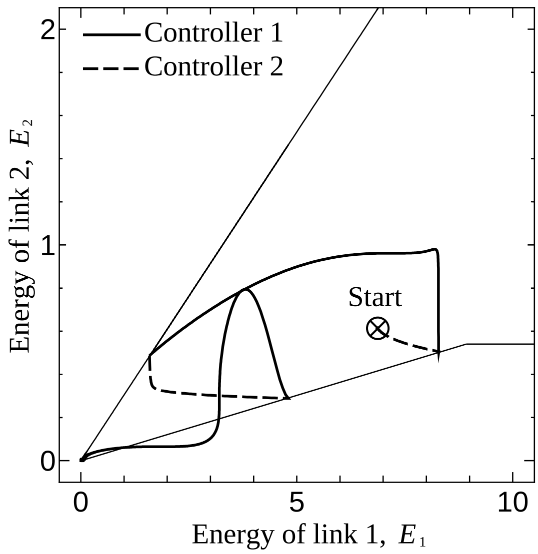

Fig. 13. Test simulation result with Case 4

trained by genetic algorithm. Although underactuated manipulators had high sensitivity to initial states in general, we obtained satisfactory results for all test conditions, according to the proposed switching method. It is concluded that the proposed method can find out an attractive domain on the energy plane.

REFERENCES

[1] Y. Nakamura, T. Suzuki, and M. Koinuma, "Nonlinear behavior and control of a nonholonomic free-joint manipulator," *IEEE Trans. on Robotics and Automation*, vol. 13, no.6, pp. 853–862, 1997.

[2] H. Arai, K. Tanie, and N. Shiroma, "Nonholonomic control of a three-DOF planar underactuated manipulator," *IEEE Trans. on Robotics and Automation*, vol. 14, no. 5, pp. 681–695, 1998.

[3] I. Fantoni, R. Lozano, and M. W. Spong, "Energy based control of the pendubot," *IEEE Trans. on Automatic Control*, vol. 45, no. 4, pp. 725–729, 2000.

[4] L. Udawatta, K. Watanabe, K. Izumi, and K. Kiguchi, "Control of underactuated manipulators using fuzzy logic based switching controller," *J. of Intelligent and Robotic Systems*, vol. 38, pp. 155–173, 2003.

[5] J. P. Hespanha and A. S. Morse, "Stabilization of nonholonomic integrators via logic-based switching," *Automatica*, vol. 35, pp. 385–393, 1999.

[6] I. Duleba and J. Z. Sasiadek, "Nonholonomic motion planning based on Newton algorithm with energy optimization," *IEEE Trans. on Control Systems Technology*, vol. 11, no. 3, pp. 355–363, 2003.